pagepress

Journal of Agricultural Engineering

Journal of Agricultural Engineering 2026; LVII:2146
doi:10.4081/jae.2026.2146

©Copyright: the Author(s), 2026
Licensee PAGEPress, Italy

Optimization of energy use and torque in vertical axis rotary tillers: effects of disc diameter and blade number on tillage performance

Artur Altunyan, Arshaluys Tarverdyan

Scientific Research Institute for Agricultural Mechanization and Automation, Armenian National Agrarian University, Yerevan, Armenia

Abstract

Efficient soil management in vineyards with stony, loamy–sand soils is crucial for energy conservation and sustainable production, particularly in organic systems where herbicide use is restricted. Rotary tillers with vertical axes are widely used for intra-row and near-trunk tillage but are often limited by high energy demand. This study aimed to develop a mathematical model to optimize the operating regime of rotary tillers by evaluating the relationship between torque resistance, which is the key energy indicator, and primary kinematic parameters: disc angular speed and diameter. Field experiments were conducted at the Voskehat Experimental Station in Armenia using a two-factor, second-order central composite design. Torque was measured with a high-precision strain-gauge system, and two groups of L-shaped blades (Z_1=3 and Z_2=4) were tested. Regression analysis showed that disc diameter had a strong linear effect on torque, while angular speed exhibited a weaker influence that varied with blade number. In all cases, torque variation did not exceed 10 N·m within the speed range of 16.5-20.5 rad s^{-1}. Distinct functional patterns of torque variation were observed depending on blade number, likely reflecting the interaction between soil deformation wave propagation and disc rotation. Defining the optimal operating regime, therefore, requires minimizing torque while ensuring that the kinematic parameters satisfy agrotechnical requirements, thereby preventing excessive soil pulverization, reducing erosion risk, and ensuring high-quality tillage.

Key words: rotary tiller; torque characteristics; vertical axis; angular speed; energy efficiency; blade quantity.

Correspondence: Artur Altunyan, Scientific Research Institute for Agricultural Mechanization and Automation, Armenian National Agrarian University, 74 Teryan Str., 0009 Yerevan, Armenia. E-mail: arturaltunyan@gmail.com

Introduction

According to the International Organization of Vine and Wine (2024), vineyards cover over 7.2 million hectares globally, with a significant concentration in semi-arid Mediterranean regions where viticulture constitutes a key economic sector (2024). In the Republic of Armenia, grape production represents a vital component of the agricultural landscape. Vineyards are primarily established on loamy-sand textured soils, which are typically characterized by a high degree of stoniness. While stony soils can positively influence grapevine root system and enhance yield quality, they simultaneously present substantial challenges for soil management and mechanized operations. Tillage of both intra-row and near-trunk vineyard zones ranks among the most labor-intensive, energy-demanding, and agronomically essential tasks within vineyard mechanization systems. From an energy standpoint, these operations may account for approximately 40-50% of the total energy input required for vineyard maintenance (Manaenkov, 2010). Mechanized soil tillage methods offer substantial advantages both economically by enhancing energy efficiency, production outcomes - crop yield and quality and technically, by ensuring the execution of high-standard agrotechnical procedures. Moreover, they enable timely implementation of field operations in accordance with optimal agronomic schedules.

In contemporary vineyard management systems, tillage of both intra-row and near-trunk zones remains a fundamental agronomic operation (Ferrero *et al.*, 2005; Hegazy *et al.*, 2014; Abo-Habaga, 2018; Peruzzi, 2017, Smart *et al.*, 2006, Manzone, 2020). As demonstrated by researchers (Martínez *et al.*,2008), conventional tillage practices may, under specific conditions, more effectively promote plant root system development compared to no-tillage approaches. Although no-tillage systems generally improve certain physical properties of the soil, these improvements are predominantly confined to the uppermost 5 cm of the soil profile. Inadequate soil aeration, especially oxygen limitation, impairs root development in compacted soils (McArtney and Ferree, 1999; Czyź, 2004; Watson and Kelsey, 2006) and does not have a negative impact on the biomass of the soil (Faber, 2017). Root oxygen uptake is governed by both soil oxygen availability and soil-rhizosphere physical conditions, which are substantially influenced by tillage practices (Bhandral *et al.*, 2007; Abu-Hamdeh, 2000; Ozpinar *et al.*, 2018). In mechanized tillage systems, energy consumption remains a critical consideration, particularly given that soil tillage alone may represent approximately 29-59% of the total fuel consumption in agricultural production (Sarauskis *et al.*, 2017; Mamkagh, 2018; Varani, 2023). Consequently, identifying the optimal operating regime for tillage implements and associated machinery is vital to ensure technological efficiency while minimizing energy input. A considerable number of theoretical and empirical investigations have addressed this objective (Ahmadi, 2017; Tarverdyan *et al.*, 2024; Damanauskas and Janulevičius, 2022; Zimmermann *et al.*, 2023, Yuan *et al.*, 2023). In the context of viticulture soil management, several studies have focused on establishing functional relationships between power demand

parameters and the operational regimes of rotary tillers of both vertical- and horizontal-axis types used in intra-row and near-trunk cultivation. Notably, the dependence of shaft torque on operational variables such as the angular speed of the tillage implement and the forward travel velocity has been extensively analyzed (Tarverdyan *et al.*, 2017). In addition, other studies have explored the influence of tillage depth on energy consumption, along with other mechanical and soil-related factors, including ballast weight, tire inflation pressure, and soil aggregate characteristics (Mamkagh, 2018; Varani, 2023, Upadhyay and Raheman, 2020).

Acknowledging the agronomic relevance of rotary tiller application particularly its positive influence on soil physical-mechanical properties, crop productivity, and mechanization efficiency a compelling need arises to optimize operating regimes and identify the key controlling parameters for field-scale application. Although various studies have addressed the energy requirements of tillage systems and their effects on soil structure, the resulting data are often fragmented or limited in scope, typically focusing on specific machine types, especially for rotary tillers with horizontal rotational axes (Amantayev *et al.*, 2025; Zhang *et al.*, 2019), and restricted soil classifications. Thus, there are still critical shortages left behind the study scope related to integrated field-based data for rotary tillers with vertical rotational axes that quantitatively characterize the relationship between resistant torque and key operational parameters, especially for vineyard systems under the loamy-sand soil conditions.

This study aims to bridge that gap by experimentally establishing and validating the relationship between a core energy indicator of rotary tillage, the torque transmitted through the tractor's PTO and the primary kinematic and operational variables (disc rangular speed and disc diameter) governing tillage dynamics for rotary tillers with vertical rotational axes. The overarching objective is to reduce energy consumption during tillage while identifying the specific parameter values and interdependencies that optimize agrotechnical performance.

The outcomes of this research are expected to inform the design of more energy-efficient tillage implements and to support sustainable vineyard soil management practices, particularly in the contexts of facing labor shortages or regulatory limitations in chemical weed control.

Materials and Methods

In horticultural land management, particularly in compacted and heavy soils, as well as in technically sensitive zones such as intra-row and near-trunk areas, rotary tillers with vertical rotational axes are widely regarded as indispensable tools (Kupryashkin and Gusev, 2020; Konstantinov, 2019). However, their extensive adoption is hindered by high energy requirements, especially when compared to alternative machines that operate based on different mechanical principles (Manaenkov, 2010; Panov and Tokushev, 2005; Sineokov and Panov, 1977). To mitigate this limitation, a range of theoretical and experimental studies have been undertaken with the objective of identifying key factors influencing resistant torque, and determining their optimal values to reduce energy consumption without compromising agrotechnical performance (Tarverdyan *et al.*, 2017; 2024, Grigoryan and Altunyan, 2021).

A series of comprehensive field-based experimental investigations were conducted under real-world operational conditions. The object of the study is the interaction between the horticultural rotary tiller and the soil environment, while the subject of the study is the machine's energy performance indicators, in particular torque (Y). The energy efficiency of rotary tillers is influenced by several kinematic and geometric parameters, including travel velocity (V_t), blade angular speed (ω), peripheral blade velocity (V_0), the kinematic regime index ($\lambda=V_0/V_t$), tillage depth (h), disc diameter (D=2R), number of blades per disc (Z), and the cutting angle (β), among others (Ahmadi, *et al.*, 2017; Panov and Tokushev, 2005).

Torque was selected as the key optimization parameter, as it facilitates an integrated assessment of technological, operational, and structural factors influencing system performance. The variation intervals for the selected independent variables were established based on an extensive review of relevant scientific literature and the practical limitations associated with field implementation (Table 1).

The selection of independent variables was informed by prior theoretical modeling and an in-depth review of the scientific literature (Zhang *et al.*, 2022; Mi *et al.*, 2025; Zhao *et al.,* 2020). For instance, Marenya and du Plessis, (2006) reported a linear correlation between torque and tillage depth, while emphasizing that working width may exert an even greater influence than depth alone. Based on these insights, the disc angular speed (X_1) and disc diameter (X_2) were selected as independent variables due to their pronounced impact on both torque generation and the overall power requirements of the rotary tiller (Tarverdyan *et al.*, 2017; Marenya and du Plessis, 2006; Ahmadi, 2017). The experimental trials were organized into two groups, with the number of blades configured as $Z_1=3$ and $Z_2=4$, respectively. All factors were carefully controlled and monitored throughout the trials. Torque values were recorded in absolute terms, and for analytical consistency, average peak values within defined time intervals were extracted for subsequent evaluation. Since the experiments were conducted under real field conditions, this methodology enables to evaluate the acting forces within the range of their maximum values. This has important practical significance and, with high accuracy represents the force conditions encountered in the real environment, which is also essential for subsequent analysis.

Thus, a two-factor, second-order experimental design was implemented in two stages, where the number of blades (Z_1 and Z_2) was varied. To reveal the functional relationship between the optimization parameter (Y) and the influencing factors (X_1 and X_2), a second-order, two-variable polynomial equation was employed:

Table 1. Levels of factor variation.

Plan matrix parameters	Coded value	Angular speed of the rotary tiller, ω (X1), (rad s^{-1})	Diameter of the rotary tiller disc, D (X_2), (mm)
Range of variation	-	2	50
Basic (zero) level	0	18.5	350
Upper level	+1	20.5	400
Lower level	-1	16.5	300

OPEN ACCESS

$$Y = b_0 + b_1X_1 + b_2X_2 + b_{12}X_1X_2 + b_{11}X_1^2 + b_{22}X_2^2 \quad \text{(Eq. 1)}$$

The domain of the selected factors, along with their values in both natural and coded forms, as well as the ranges of variation, are presented in Table 1. From now on, the values of the factors presented in all figures and graphs, which will be presented in coded form, must be recalculated in accordance with the values given in Table 1.

An orthogonal central composite design (CCD) was employed for the experimental framework, comprising n=9 experimental runs, which included n_0=1 center point and n=3 replications per experimental condition, resulting in a total of 27 experimental trials. This design structure was chosen to ensure optimal spatial coverage of the factorial domain and to enhance statistical robustness.

Experimental sites and soil characteristics

The field experiments were conducted at the Voskehat Experimental Station of the Armenian National Agrarian University (ANAU) (Figure 1), which is located in the Ararat Valley of the Republic of Armenia, at an elevation of approximately 1000 m above sea level, where the soil cover consists of irrigated meadow soil, gray in color, with medium humus content, calcareous properties, and a loamy-sand textural composition. The coefficients $K_{1.5}$ and K_V characterize the mechanical properties of the soil as influenced by the deformation rate, have the following values for the soils of orchards and vineyards in the Republic of Armenia: $K_{1.5}$=(2.1-3.7) × 10^4 N/m^2 and K_V=(0.3-0.8) × 10^4 N s/m^3 (Tarverdyan *et al.,* 2017; He *et al.,* 2025). Based on the soil type and physical-technological properties of the experimental field, in the frontal (cutting) zone of the rotor, the values were $K_{1.5}$=2.9 × 10^4 N/m² and K_V=0.6 × 10^4 N s/m^3. In the rear zone, corresponding to the already loosened soil, the values were $K_{1.5}$=2.09 × 10^4 N/m^2 and K_V=0.42 × 10^4 N s/m^3.

Experimental setup and measure sensors

The experimental setup utilized a dual-disc rotary tiller featuring a vertical axis of rotation. An MTZ-1212 tractor served as the traction unit, operating at forward speed 4.0 km/h, thereby encompassing the high-efficiency tillage regime typically observed at speeds exceeding 3.0 km/h. Torque at the input shaft of the rotary tiller designated as the key optimization parameter was continuously monitored using high-precision torque sensor integrated with an analog-to-digital conversion module of the ZetLAB system (Figure 1b). For this purpose, a TRA-50K torque sensor was utilized (Figure 1c), ensuring accurate and reliable measurement of mechanical loading (Table 2). The recording of data was carried out at a frequency of 10Hz.

Rotational motion was transmitted from the tractor's power take-off (PTO) through a bevel gearbox (i_1=2) and a chain transmission system (i_1=29/19) , resulting in a final transmission ratio of k=i_1 × i_2=3.05. This ratio was accounted for in all subsequent calculations of mechanical power. As for the rotation speed of the rotary tiller disc, it was regulated by an independent PTO of the tractor, which was carried out from the tractor cabin using a manual mechanical adjustment lever, which could be fixed in the desired position, and the required rotation speed was set on the rotary tiller disc using a tachometer.



a)



b)



c)

Figure 1. The experimental rotary tiller in field test. **a**) Experimental implement. **b**) Analog-to-digital converter of the ZetLAB TRA-50K torque sensor used for torque resistance measurement (**c**).

To capture the actual torque exerted on the tiller, a torque sensor was installed between the PTO output and the input shaft of the bevel gearbox (Figure 1). For improved measurement accuracy, L-shaped blades were mounted exclusively on one of the rotary discs, while the second disc remained inactive. This configuration enabled precise isolation and evaluation of the torque acting on a single working disc, thereby ensuring more accurate and representative assessments of mechanical power demand (Figure 1a).

The L-shaped blades featured a bend angle of 15°, a thickness of 8 mm, and a sharpening angle of δ =20°. The working depth was set at h=8 cm. Both feed rate and chip thickness were left uncontrolled in order to allow for a broader exploration of variable interactions and to reflect more realistic field variability within the experimental factor space.

From the geometric and kinematic characteristics of the rotary tiller used in the field tests that are given in Table 3, where the kinematic working parameter (λ) is also indicated, we can see that its range is from 2,11 to 3,49.

And as

$$\lambda = \frac{V_0}{V_t} = \frac{2\pi R}{SZ} \text{ and } S = \frac{2\pi R}{\lambda Z} \quad \text{(Eq. 2)}$$

where S is a feed size (m), R is the radius of the rotary tiller disc (m), Vt is the forward velocity of the tractor (m/s), V_0 is the peripheral speed of the blade (m/s), λ is the kinematic parameter of a rotary tiller, Z is the number of blades per disc; therefore, S range is from 7 to 19.8 cm. This range fully satisfied the agrotechnical requirements for rotary tillers designed to work on loamy–sand soils (Sineokov and Panov, 1977). The minimum value occurs for Z=4 blades, when S=7-14 cm.

To accommodate experimental variation in both the number of blades and disc diameters, three custom-fabricated rotary discs were manufactured with diameters of D=300; 350 and 400 mm. Each disc was precisely machined with pre-defined blade mounting holes, strategically positioned to support both three-blade and four-blade symmetric configurations. This design ensured that the angular spacing of the blades remained consistent and geometrically accurate, regardless of the configuration used (Figure 2).

The coefficients of the selected regression model (Eq. 1) were estimated using the least squares method, implemented *via* SPSS statistical analysis software and summarized in the ANOVA results table. For each regression coefficient, the corresponding variance and confidence interval were calculated based on Student's *t*-test. Coefficients that failed to meet the predefined significance threshold (γ=0.05) were not excluded from the final model formulation to allow comparison of their relative values and influence. The overall adequacy and statistical validity of the resulting regression model were evaluated using Fisher's F-test.

Results and Discussion

Since the experiments were conducted in two distinct groups differing in the blade numbers of, the results are presented separately for the trials with Z_1=3 and Z_2=4 blades.

Experiments with Z_1=3 blades

Accordingly, for the first experimental group consisting of Z_1=3 blades and n=3 replications per treatment condition, the torque measurements used as the response variable, were processed and statistically analyzed using SPSS statistical analysis software, resulting in the summary data presented in Tables 4 and 5. As presented in Table 4, the estimated regression coefficients indicate the relative influence of the main factors and their interactions on the torque response.

The following Table 5 summarizes the ANOVA results obtained from a numeric regression model applied to the Z_1=3



Figure 2. General view of the rotary tiller experimental disc used in the experiments (example D = 400 mm).

Table 2. Specifications for torque sensor TRA-50K (Dacell Co., Cheongju-si, Korea).

Specifications for torque sensor TRA-50K	Accuracy
Rated capacity (RC)	50kgf-m (490.3 N-m)
Rated output (RO)	1.5mV/V±1% (1~5 kg f-m:1mV/V)
Nonlinearity	0.3% from RO
Hysteresis	0.2% from RO
Terminal resistance	350Ω±1%
Insulation resistance bridge	200MΩ
Temperature effect, on rated output	0.2% Load/10°C
Temperature effect, on zero balance	0.3% from RO /10°C
Safe overload	120% from RC

OPEN ACCESS

experimental configuration. The model includes main effects (X_1, X_2) and their interaction ($X_1 \times X_2$).

$$Y = 86.387 + 1.578 \cdot x_1 + 9.791 \cdot x_2 + 3.532 \cdot x_1 x_2 - 2.260 \cdot x_1^2 + 1.631 \cdot x_2^2$$

(Eq. 3)

The developed mathematical model (Eq. 3) allows for the calculation, prediction, and optimization of torque values as a function of the identified influencing factors, within the investigated experimental region . The overall model was statistically significant (F=5.836, p=0.00157), indicating that the fitted model explains a significant proportion of the observed variation in the response. Analysis of the regression model (Eq. 3) and the corresponding response surface plots illustrating the functional relationship Y=f (X_1, X_2) (Figures 3 and 4) indicates that the diameter of the rotary disc exerts a statistically highly significant and dominant influence (p<0.0001) on torque magnitude (Table 5). Even slight variations in disc diameter led to a linear and measurable impact on the power-related characteristics. In contrast, the effect of angular speed (X_1) exhibited a primarily quadratic trend (Figure 4b). Although increasing the rotational speed does result in higher torque values from a power-engineering perspective, the relative magnitude of this effect is notably smaller compared to that of the disc diameter, as confirmed by the standardized regression coefficients. For example, the amplitude of this quadratic effect remains relatively limited, not exceeding 10 N·m when the angular speed ranges from 16.5 rad s^{-1} to 20.5 rad s^{-1} (Figure 4b), which may be considered negligible from the perspective of total energy expenditure.

According to the ANOVA results (Table 5), factor X_1 (p=0.4240) and the interaction term $X_1 \times X_2$ (p=0.1510) were not

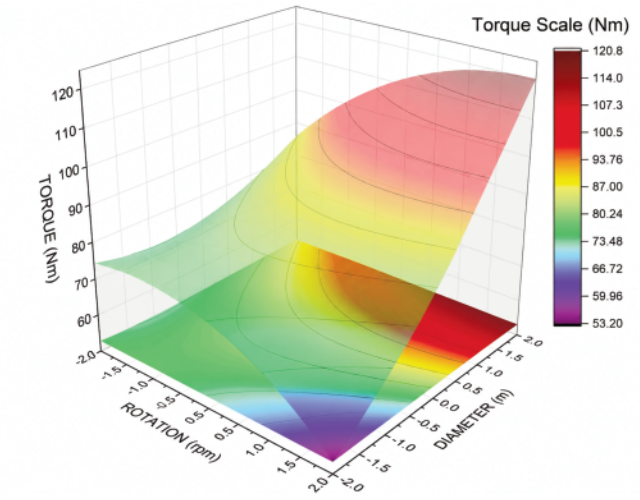


Figure 3. Response surface plot of resistant torque (N·m) as a function of angular speed (X_1, [rad s^{-1}]) and disc diameter (X_2, [mm]), for Z_1=3 blade.

Table 3. Values of the kinematic working parameter (λ) as a function of experimental factors (ω, D), under the condition of a constant forward travel velocity of the aggregate V_t =4.0 km/h.

Angular speed of the rotary tiller disc (rad s^{-1})	Values of the kinematic parameter (λ) Disc diameters (mm) D_1=300	D_2=350	D_3=400
ω_1=16.5	2.11	2.46	2.82
ω_2=18.5	2.37	2.76	3.16
ω_3=20.5	2.61	3.05	3.49

Table 4. Regression coefficient estimates and 95% confidence intervals for the quadratic model.

Parameter	Estimate	Std. error	95% Confidence interval Lower bound	Upper bound
b0	86.387	3.5326	79.0408	93.7338
b1	1.578	1.9349	-2.4461	5.6016
b2	9.791	1.9349	5.7667	13.8144
b12	3.532	2.3698	-1.3966	8.4598
b11	-2.260	3.3513	-9.2290	4.7100
b22	1.631	3.3513	-5.3381	8.6009

Table 5. Analysis of variance (ANOVA) for the Z_1=3 experiment.

Source	Sum of squares	df	F-value	p
X1	44.8071	1	0.6649	0.4240
X2	1725.3796	1	25.6033	0.000052
X1:X2	149.6673	1	2.2209	0.1510
$X1^2$	30.6327	1	0.4546	0.5075
$X2^2$	15.9687	1	0.2370	0.6315
Residual	1415.1702	21	-	-

statistically significant. The quadratic effects (p=0.5075) and (p=0.6315) were not statistically significant at the 95% confidence level, suggesting limited evidence of curvature within the investigated experimental region. These findings indicate that X_2 plays a dominant role in determining the system output under the conditions tested. Therefore, this interpretation should be considered as a hypothesis requiring further experimental validation.

An important observation relevant for both research and practical application concerns the interaction between disc diameter and angular speed. For larger rotary discs (D=400 mm), torque increases with angular speed, whereas for smaller discs (D=300 mm), higher angular speed reduces torque (Figure 4b). These relationships apply only within the tested speed range; outside this interval, the response may differ. Notably, from approximately D=375 mm (Figure 4b), increasing angular speed may also reduce torque, even for larger discs. This behavior suggests the presence of a transitional zone in which the effect of rotational speed on torque approaches linearity at a specific disc diameter. This critical diameter or interval may be defined as a "breakpoint domain." The shift in torque response is likely associated with interactions between soil deformation wave propagation, cutting velocity, and speed-dependent changes in soil deformation during the cutting process.

Experiments with Z_2=4 blades

For the second group of experiments (Z_2=4 blades), with the same number of replications (n=3), a final regression model (Eq. 4) for the measured torque values was developed using SPSS statistical analysis software, resulting in the summary data presented in Tables 6 and 7.

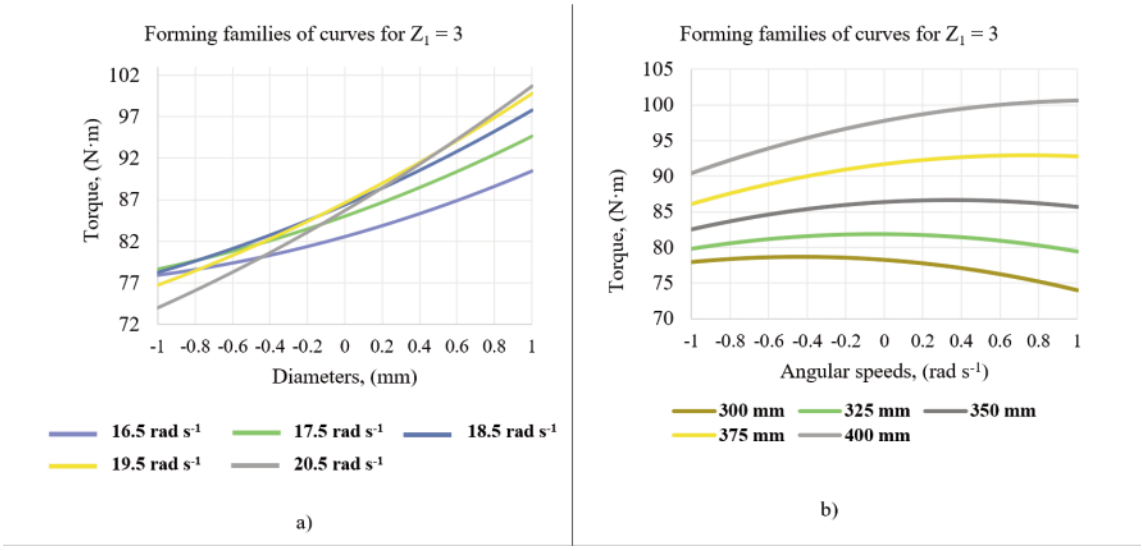


Figure 4. Set of curves for Z_1=3 blade illustrating the relationship between rotary tiller torque and disc diameter, when angular speed is constant (**a**); angular speed, when disc diameter is constant (**b**).

Table 6. Regression coefficient estimates and 95% confidence intervals for the quadratic model.

Parameter	Estimate	Std. error	95% Confidence interval	
			Lower bound	Upper bound
b0	86.057	2.1793	81.5246	90.5886
b1	.063	1.1936	-2.4190	2.5455
b2	17.956	1.1936	15.4736	20.4381
b12	1.412	1.4619	-1.6277	4.4526
b11	1.439	2.0674	-2.8602	5.7386
b22	-5.745	2.0674	-10.0446	-1.4457

Table 7. Analysis of variance (ANOVA) for the Z_2=4 experiment.

Source	Sum of squares	df	F-value	p
X1	0.0720	1	0.0028	0.9582
X2	5803.4169	1	226.2946	<0.0001
X1:X2	23.9414	1	0.9336	0.3449
$X1^2$	12.4278	1	0.4846	0.4940
$X2^2$	198.0384	1	7.7222	0.0112
Residual	538.5534	21	—	—

OPEN ACCESS

$$Y = 86.057 + 0.06327 \cdot x_1 + 17.9556 \cdot x_2 + 1.4125 \cdot x_1 x_2 + 1.43921 \cdot x_1^2 - 5.74511 \cdot x_2^2$$

(Eq. 4)

The overall model was statistically highly significant (F=47.09, p<0.0001), demonstrating strong predictive capability. The following table presents the ANOVA results derived from the numeric regression model applied to the Z_2=4 factorial design. The analysis (Table 7) includes the main effects of X_1 and X_2 and their interaction.

Analysis of the derived regression model (Eq. 4), along with the corresponding response surface plots Y=f (X_1, X_2) (Figures 5 and 6), confirms that, in this experimental group as well, the diameter of the rotary tiller disc (X_2) exerts a highly significant influence on torque generation (p<0.0001). Even minor changes in disc diameter produce a clearly linear and pronounced effect on torque-related characteristics. The disc's angular speed (X_1), consistent with the observations in the Z_1=3 blade configuration, exhibits a relatively low influence (p=0.9582), and was identified as the least influential factor. However, the amplitude of this effect remains relatively limited, not exceeding 5 N·m when the angular speed ranges from 16.5 s^{-1} to 20.5 s^{-1} (Figure 6b), which may be considered negligible from the perspective of total energy expenditure. Therefore, within this operational interval (Table 2), the selection of angular speed can be guided primarily by agrotechnical considerations -such as the desired geometric characteristics of the processed soil fraction, the risk of excessive pulverization, the definition of kinematic regimes, and other field-specific requirements. Analysis of the curves showed that, with four blades (Z_2=4), torque remained nearly constant across the tested angular speed range (Figure 6b). This stability promotes smooth and consistent tillage operation, improving the rotary tiller's reliability, mechanical durability, and tillage quality.

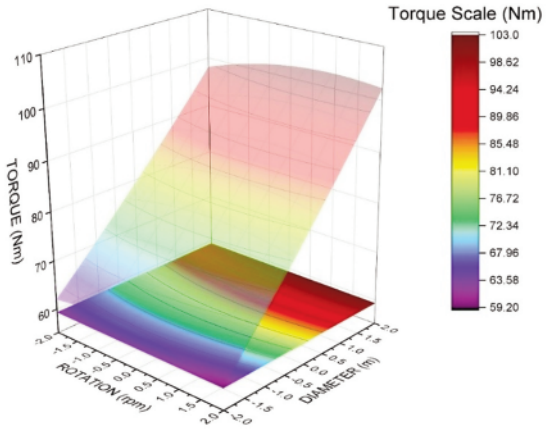


Figure 5. Response surface plot of resistant torque (N·m) as a function of angular speed (X1, [rad s^{-1}]) and disc diameter (X_2, [mm]), for Z_2=4 blade.

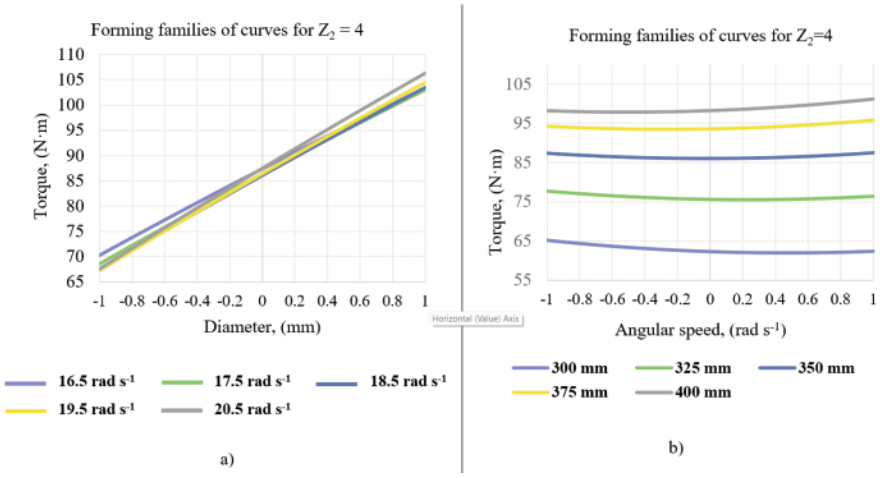


Figure 6. Set of curves for Z2=4 blade illustrating the relationship between rotary tiller torque and disc diameter, when angular speed is constant (**a**); angular speed, when disc diameter is constant (**b**).

Table 8. Values of the kinematic working parameter (λ) as a function of experimental factors (ω, D), assuming a constant forward travel velocity of the aggregate V_t =2.6 – 3.0 km/h.

Angular speed of the rotary tiller disc (rad s_{-1})	Values of the kinematic parameter (λ) Forward travel velocity of the aggregate (m·s^{-1})	Disc diameters (mm) D_1=300	D_2=350	D_3=400
ω_1=16.5	0.722	3.43	4.00	4.57
	0.833	2.97	3.47	3.96
ω_2=18.5	0.722	3.84	4.48	5.12
	0.833	3.33	3.89	4.44
ω_3=20.5	0.722	4.24	4.94	5.65
	0.833	3.67	4.29	4.90

Using the regression formulae (Eqs. 3 and 4), the resistance torque required for the operation of one disc of the rotary tiller can be calculated by multiplying the obtained result by the gear ratio of the machine (k=3.05). For example, for Z_1=3 the minimum resistance torque is M_{min}=74.013 N·m. This means that for the operation of one disc with D=300 mm and ω=20.5 rad s^{-1}, the required resistance torque will be M_{min}= 74.013 ·3.05=225.74 N · m, assuming all other operating parameters are identical to those used during the experiment. Although the obtained parameter values and their operational ranges are technically acceptable and demonstrate improved energy efficiency, and no adverse tillage performance was observed in field experiments conducted using the selected parameter values, agrotechnical requirements must also be regarded as essential regulatory benchmarks. A critical limitation emerges when the tractor operates at relatively high forward velocity, resulting in blade trajectories that fail to intersect the root systems of weed residues effectively. This constraint is particularly evident in rotary tillers designed for intensive orchard and vineyard cultivation, where disc diameters typically range between 200-400 mm and the peripheral velocity may be insufficient to ensure effective soil cutting. Optimization of the rotary tiller kinematic regime must consider environmental and operational conditions. Because angular speed is largely predetermined and excessive values may increase soil pulverization, tractor forward velocity remains the primary adjustable parameter for meeting agrotechnical requirements. For the developed rotary tiller under the heavy and loamy-sand soils typical of the Republic of Armenia, the recommended operating parameters are: chip thickness δ=2.5-3.0 cm; disc radius r=150-200 mm; angular velocity ω=16.0-17.8 rad s^{-1} (n=150–170 rpm); tractor velocity V_t=2.6–3.0 km/h, and kinematic parameter λ=3.0...5.12 (Table 8). Angular speeds higher than 17.8 s^{-1} are undesirable because of erosion risk, whereas lower speeds reduce tillage quality and weed-root cutting efficiency.

Beyond these practical considerations, torque behavior differed markedly between blade configurations (Z_1=3 and Z_2=4) (Figures 4b and 6b). The Z_1=3 configuration showed a downward-opening parabolic trend, while Z_2=4 exhibited an upward-opening trend, likely reflecting interactions between soil deformation wave propagation and blade peripheral velocity. This phenomenon may be interpreted as resulting from the interaction between deformation wave propagation in the soil medium and the peripheral velocity of the cutting blades.

In the Z_1=3 configuration, torque reached a minimum when deformation and cutting velocities approached equilibrium and increased at higher blade speeds. Increasing blade number improved energy transfer efficiency and reduced torque per blade. While this interpretation is theoretically grounded, further experimental validation of this mechanism is required. Based on the results of scientific experiments and the conducted analyses, a universal horticultural rotary tiller (Figure 7) was designed and manufactured. For its working elements and kinematic parameters, the following values were selected: D=400 mm, Z=4, ω=15.7…16.8 s^{-1}, V_t=2.6…3.0 km/h. The machine underwent field testing at one of the largest viticulture enterprises in Armenia (40°09'45.2"N 43°51'37.1"E), demonstrating high-quality performance and operational reliability. The obtained soil tillage parameters satisfied the applicable agricultural requirements.



Figure 7. An industrial prototype of a universal rotary tiller developed by a scientific team (ANAU).

Conclusions

Within the framework of this investigation, a comprehensive examination was conducted on the energetic and kinematic characteristics of rotary tillage implements with vertical axes of rotation, specifically intended for use in horticultural soils of heavy and loamy–sand physical–mechanical composition. Based on rigorously designed field experiments employing L-shaped blades in two configurations (Z_1=3 and Z_2=4), and supported by regression modeling, the interrelationship between torque resistance, recognized as the principal energetic indicator of such implements, and the key influencing parameters – disc diameter and angular speed was systematically evaluated.

The results demonstrated that disc diameter exerts a dominant linear effect on torque, independent of blade number and angular speed. In contrast, angular speed contribution to the overall energy demand was negligible. The patterns of these graphs differed depending on the number of blades. This indicates the presence of complex interactions between the rotary tiller blades and the soil during operation, the elucidation of which requires a detailed investigation, with particular attention to the relationship between the propagation velocity of deformation waves in the soil and the angular speed under varying blade numbers. Understanding this phenomenon is key to analyzing energy use and optimizing implement performance. Torque reduction should be seen not just as a kinematic effect but as a result of soil-tool interactions, allowing factor values to be adjusted accordingly. Designing such implements requires defining an optimal operating regime that minimizes torque while meeting agrotechnical needs. This prevents excessive soil pulverization, reduces erosion, and ensures quality tillage.

References

Abo-Habaga M, Imara Z, Okasha M, 2018. Development of a combine hoeing machine for flat and ridged. J Soil Sci Agric Eng 9:817-820.

Abu-Hamdeh NH, 2000. Effect of tillage treatments on soil thermal conductivity for some Jordanian clay loam and loam soils. Soil Till Res 56:145-151.

Ahmadi I. 2017. A power estimator for an integrated active-passive tillage machine using the laws of classical mechanics. Soil Till Res 171:1-8.

Bernacki H, 1962. [Theory of Tillers].[Article in Polish]. Warsaw, Institute of Agricultural Mechanization and Electrification.

OPEN ACCESS

Bhandral R, Saggar S, Bolan NS, Hedley MJ, 2007. Transformation of nitrogen and nitrous oxide emission from grassland soils as affected by compaction. Soil Till Res 94:482-492.

Czyż EA, 2004. Effect of traffic on soil aeration, bulk density and growth of barley. Soil Till Res 79:153-166.

Damanauskas V, Janulevičius A, 2022. Effect of tillage implement (spring tine cultivator, disc harrow), soil texture, forward speed, and tillage depth on fuel consumption and tillage quality. J Agric Eng 53:1371.

Faber F, Wachter E, Zaller JG, 2017. Earthworms are little affected by reduced soil tillage methods in vineyards. Plant Soil Environ 63:257-263.

Ferrero A, Usowicz B, Lipiec J, 2005. Effects of tractor traffic on spatial variability of soil strength and water content in grass covered and cultivated sloping vineyard. Soil Till Res 84:127-138.

Grigoryan AS, Altunyan AV, 2021. [The effect of some factors on the cutting angle of the vertical blade during rotary soil tillage].[Article in Armenian with English abstract]. AgriSci Technol 75:230-23.4

He C, Han G, Ye T, Wei M, Sun C, Cheng Y, 2025. Design and evaluation of a new deep vertical rotary tiller for enhanced field performance. INMATEH Agric Eng 76:746-756.

Hegazy RA, Abdelmotaleb IA, Imara ZM, Okasha MH, 2014. Development and evaluation of small-scale power weeder. Misr J Agric Eng 31:703-728.

International Organisation of Vine and Wine, 2024. State of the World Vine and Wine Sector in 2024. Available from: https://www.oiv.int/sites/default/files/2025-04/OIV-State_of_the_World_Vine-and-Wine-Sector-in-2024.pdf

Konstantinov YU, 2019. [Calculation method of resistance and resistance moment to the soil cutting with a straight disc blade of the cutter].[Article in Russian with English abstract]. Tract Agric Mach 86:31-39.

Kupryashkin VF, Gusev AY, 2020. [Justification of the parameters and operating modes of a self-propelled soil cultivation cutter with the combined rotation of the active working tools] [Article in Russian]. Sci Rev Int Sci Pract J 2:42-48.

Mamkagh AM, 2018. Effect of tillage speed, depth, ballast weight and tire inflation pressure on the fuel consumption of the agricultural tractor: a review. J Eng Res Rep 3:1-7.

Manaenkov KA, 2010. [Resource-saving technologies and a complex of machines for soil care in intensive gardens].[Thesis Diss. in Russian]. Moscow.

Manzone M, Demeneghi M, Marucco P, Grella M, Balsari P, 2020. Technical solutions for under-row weed control in vineyards: Efficacy, costs and environmental aspects analysis. J Agric Eng 51:991.

Marenya MO, du Plessis HLM, 2006. Torque requirements and forces generated by a deep tilling down-cut rotary tiller. Paper 061096 in Proc. ASABE Annual Meeting, St. Joseph

Marenya MO, du Plessis HLM, 2007. Modelling torque and power requirements for a deep tilling down-cut rotavator. Paper 071125in Proc. ASABE Annual Meeting, St. Joseph.

Martínez E, Fuentes JP, Silva P, Valle S, Acevedo E, 2008. Soil physical properties and wheat root growth as affected by no-tillage and conventional tillage systems in a Mediterranean environment of Chile. Soil Till Res 99:232-244.

McArtney SJ, Ferree DC, 1999. Root and cane pruning affect vegetative development, fruiting and dry matter accumulation in grapevines. HortScience 34:617-621.

Mi J, Xie H, Niu P, 2025. Design and optimisation of rotary tiller blade for orchards in hilly mountainous areas based on the discrete element method. INMATEH Agric Eng 76:177-186.

Ozpinar S, Ozpinar A, Cay A, 2018. Soil management effect on soil properties in traditional and mechanized vineyards under a semiarid Mediterranean environment. Soil Till Res 178:198-208.

Panov IM, Tokushev ZE, 2005. [Theory, design and calculation of rotary tilling machines].[Book in Russian]. Kokshetau, Publ. Press of Kokshetau University.

Peruzzi A, Martelloni L, Frasconi C, Fontanelli M, Pirchio M, Raffaelli M, 2017. Machines for non-chemical intra-row weed control in narrow and wide-row crops: a review. J Agric Eng 48:57-70.

Sarauskis E, Vaitauskiene K, Romaneckas K, Jasinskas A, Butkus V, Kriauciunien Z, 2017. Fuel consumption and CO2 emission analysis in different strip tillage scenarios. Energy 118:957-968.

Sineokov GN, Panov IM, 1977. Theory and calculation of tillage machines. Mashinostroenie, Moscow.

Smart D, Schwass E, Lakso A, Morano L, 2006. Grapevine rooting patterns: a comprehensive analysis and a review. Am J Enology Vitic 57:89-104.

Tarverdyan AP, Altunyan AV, Grigoryan AS, 2024. Rationale of the optimal shape and placement angle variation pattern of the tillage rotary blade. INMATEH Agric Eng 74:1047-1056.

Tarverdyan AP, Sargsyan SF, Altunyan AV, 2017. Investigation results of kinematic and dynamic indicators of tiller with vertical rotation axis in orchards soil cultivation. Ann Agric Sci 15:163-168.

Tarverdyan AP, Altunyan AV, Grigoryan AS, Harutyunyan GS, 2024. Dynamic-energy analysis of a rotary tiller with a vertical rotation axis. INMATEH Agric Eng 73:275-284.

Upadhyay G, Raheman H, 2020. Comparative assessment of energy requirement and tillage effectiveness of combined (active-passive) and conventional offset disc harrows. Biosyst Eng 198:266-279.

Varani M, Mattetti M, Molari G, Biglia A, Comba L, 2023. Correlation between power harrow energy demand and tilled soil aggregate dimensions. Biosyst Eng 225:54-68.

Watson G, Kelsey P, 2006. The impact of soil compaction on soil aeration and fine root density of Quercus palustris. Urban For Urban Green 4:69-74.

Yuan Y, Wang J, Zhang X, Zhao S, 2023. Study on tillage resistance and energy consumption of a plain straight rotary blade for strip tillage. Eng Agric 43:e20220127.

Zhao H, Li H, Ma S, He J, Wang Q, Lu C, et al., 2020. The effect of various edge-curve types of plain-straight blades for strip tillage seeding on torque and soil disturbance using DEM. Soil Till Res 202:104674.

Zimmermann G, Jasper S, Savi D, Francetto T, Cortez J, 2023. Full-powershift energy behavior tractor in soil tillage operation. Eng Agric 43:e20230054.

Received: 17 February 2026 Accepted: 14 July 2026.

Contributions: Artur Altunyan, conceptualization, methodology, investigation, formal analysis, data curation, writing – original draft. Arshaluys Tarverdyan, writing – original draft, writing – review & editing. All authors reviewed and approved the final version of the manuscript and agreed to be accountable for all aspects of the work.

Conflict of interest: the authors declare that they have no competing interests and all authors confirm accuracy.

Data Availability Statement: the datasets used and/or analyzed during the current study are available upon reasonable request from the corresponding author.

Funding: this work was supported by the Higher Education and Science Committee of Republic of Armenia (research project n. 21APP-2D015).

Publisher's note: all claims expressed in this article are solely those of the authors and do not necessarily represent those of their affiliated organizations, or those of the publisher, the editors and the reviewers. Any product that may be evaluated in this article or claim that may be made by its manufacturer is not guaranteed or endorsed by the publisher.

This work is licensed under a Creative Commons Attribution-NonCommercial 4.0 International License (CC BY-NC 4.0).

OPEN ACCESS